Axial Bearing Behaviour of a Model Pile in Sand Under Multiple Static Cycles

J. H. Hwang[1], Z. X. Fu[2], P. Y. Yeh[3], D. W. Chang[4]

[1,2,3]*Department of Civil Engineering, National Central University, Jhongli, Taiwan*
[4]*Department of Civil Engineering, Tamkang University, New Taipei City, Taiwan*
[1]*E-mail*: hwangin@cc.ncu.edu.tw
[2]*E-mail*: cyce14@hotamil.com
[3]*E-mail*: 953202020@cc.ncu.edu.tw
[4]*E-mail*: dwchang@mail.tku.edu.tw

ABSTRACT: This paper designed and built a set of loading equipment for conducting model pile test. The cyclic axial load was manually applied in a displacement-controlled type. A fully instrumented *aluminium* model pile was designed with the outer and inner diameters of 18mm and 17mm and a length of 450mm. The thickness is only 0.5mm. The length to diameter ratio is approximately 25. Seven strain gauges were carefully pasted on the inner wall and a mini-type load cell was installed at the bottom of the wall. The sand specimens were prepared in a relative density approximately 70% and with a diameter of 40cm and a height of 60 cm. Two types of cyclic axial load were performed for both dry sand and saturated sand. The first applies the compressive load first and then applies the uplift load. This finished a compressive-tensile load cycle(C-T type). The same cycle was then repeated five times. The second applies the uplift load first and then applying the compressive load. This finished a tensile-compressive load cycle (T-C type). Each cycle was then repeated five times also. The measured load-displacement curves of pile head and the transfer curves of the pile shaft were analysed to deduce the characteristics of cyclic axial bearing behaviours. The focus was put on (1) the difference of the compressive and tensile bearing capacities; (2) the effect of the number of applied loading cycles; (3) the development of end bearing capacity with pile head displacement; (4) the unit friction distribution pattern along pile length. Based on the test results, some interesting phenomenon and conclusions are reported herein.

1. INTRODUCTION

It has established the tensile capacity (pull out capacity) of a single pile is significantly less than its compressive capacity (e.g., Tomlinson, 1977). Nicola and Randolph (1993) conducted a detailed study on the tensile and compressive shaft capacities of piles in sands by theoretical and numerical methods. They concluded that the capacity ratio (tensile/compressive) mainly depends on the Poisson's ratios of pile and soil, the modulus ratio (Young's modulus of pile / shear modulus of soil) and pile length ratio (pile length/pile diameter). Among the relevant studies based on field pile load tests, Tomlinson (1977) indicated that the tensile capacity is approximately 50% of the compressive capacity for driven piles in sand. Mansur and Hunter (1970) showed that the tensile frictional capacity is approximately 65% of the compressive frictional capacity for driven piles in a project near Arkansas River. Beringen et al. (1979) revealed the tensile/compressive capacity ratio ranges from 0.65 to 0.76 based on the results of pile load tests. Fumio (1994) collected and analysed the nine load test data for driven piles and bored piles, and found the tensile/compressive frictional capacity ratio is approximately 0.8. Amira et al. (1995) indicated the tensile frictional capacity is less than the compressive frictional capacity based the model pile tests and the average capacity ratio is around 0.5. In Japanese code of highway (JRA, 1996), the ultimate tensile unit friction is half of the calculated compressive unit friction.

Although the above research shed valuable insights on the difference between the tensile and compressive capacities of a single pile, there is still a need for further investigation of the difference between tensile and compressive model pile load tests under well controlled conditions, i.e. using the same soil and pile. Moreover, in earthquake-active countries, the tensile and compressive bearing behaviour of a single pile in cyclic loading is more important than that in static loading. Review of the relevant literature in this field has uncovered limited research on this aspect. Expense and Difficulty to perform cyclic axial loading test in a field pile load test are possibly the justifications for limited research. Based on the above considerations, this study designed large scale model pile test equipment that could perform the static and cyclic axial loading on a model pile. Four cyclic axial pile load tests have been successfully carried out by the equipment. Two tests are for dry sands and the other two are for saturated sands.

The following study describes the design of the test equipment, sample preparation, the test procedure of the cyclic loading, the test results and analysis and finally summarizes the main findings from the tests.

2. TEST DESIGN AND PROCEDURE

2.1 Test Equipment

2.1.1 Model Test Tank

This study used three 20cm high cylinders to form a test tank of 60cm height. The bottom seat is a plate made of aluminium alloy with dimensions of 60cmx60cmx3cm. There is a cylindrical O-ring on the plate to prevent water leakage from the contact surface between cylinder and the seat. There are several porous stones on the top of the seat and a water pipe is connected to the side hole of the seat so that water can pass through the seat into the soil specimen while during consolidation or saturation process. A standpipe connecting to the side hole is used to monitor the excess pore pressure induced by pile penetration.

2.1.2 Instrumented Model Pile

Since the test tank can be regarded as a rigid wall calibration chamber, based on the previous research experiences on the boundary condition (BC) effect, the BC effect can be neglected when the diameter ratio of chamber to model pile is greater than 20. Thus, the outer diameter of the model pile is designed to be 18mm and the chamber/pile diameter ratio is approximately 23 which meet the above requirement of boundary condition.

2.1.2.1 Design of Pile Shaft

The pile shaft is designed as a hollow aluminium alloy tube with an outer diameter of 18mm and a tube thickness of 0.5mm. The total length of the model pile is 47.5cm which is assembled by a single long tube segment (45cm) and a pile tip (2.5cm), as shown in Figure 1. The strain gauges used are of an electrical resistance of $120\,\Omega$. The axial force is measured by the strain gauge connecting

to the data logger in a half bridge type. A side slot is installed on the uppermost tube segment so that the electrical wire lines connecting the strain gauges can be extended outside the pile shaft to connect the data logger.
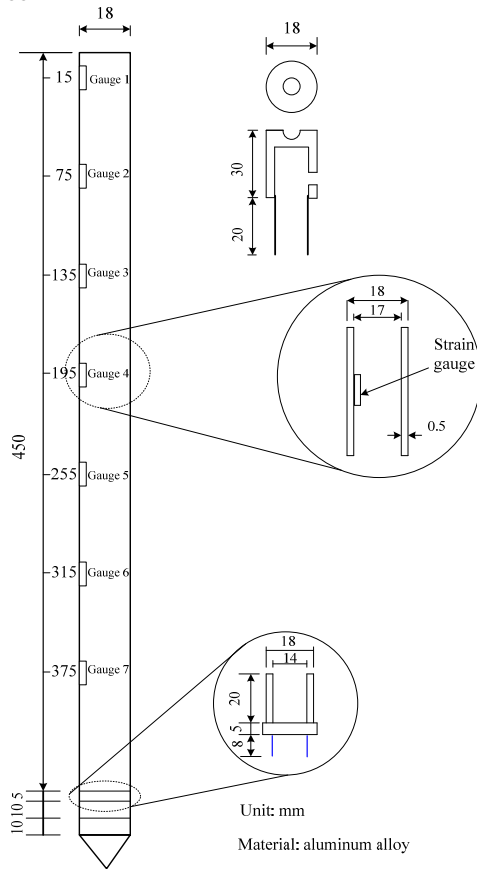

Figure 1 Design details of the model pile

Figure 2 Decomposed elements of the load cell chamber

Figure 3 The fully assembled model pile

2.1.2.2   Design of Pile Tip

To accurately measure the end bearing behavior of pile, this study designed a mini load cell at the pile bottom. The size of the load cell must be small enough to be installed into the pile and its load capacity has to sustain the maximum pile tip load encountered during pile installation and pile load test. Based on some pilot tests, the maximum load at the pile top is approximately 107.91 N during pile penetration. The resistance at the pile bottom must be less than 107.91 N. Thus, the button type load cell LBS-50 from Interface Company is selected to meet the above requirements. A water-proof cell chamber was designed to install the button load cell and its two ends were connected to the pile shaft and pile tip. The decomposed elements of the load cell chamber are shown in Figure 2 and the fully assembled model pile is displayed in Figure 3.

2.1.3   Loading Device

To apply the long-term loading, the stability and continuity of loading device are very important. Thus, this study adopted dead loads as applied loads to ensure the applied load is constant during loading period and keep its position and direction coincide with the center axis of the model pile, A steel wire line and pulley assembly plus a directional bearing ,as shown in Figure 4, was designed to apply the long-term loading. A vertical bar extended from the center of movable pulley passes through the directional bearing and connects its two ends to the load cell and butterfly clipper. The displacement gauge (LVDT) is placed on a short rigid steel strip which rests on the pile top. The lower fixed pulley set is used to apply compressive load, while the upper fixed pulley set is used to apply tensile load
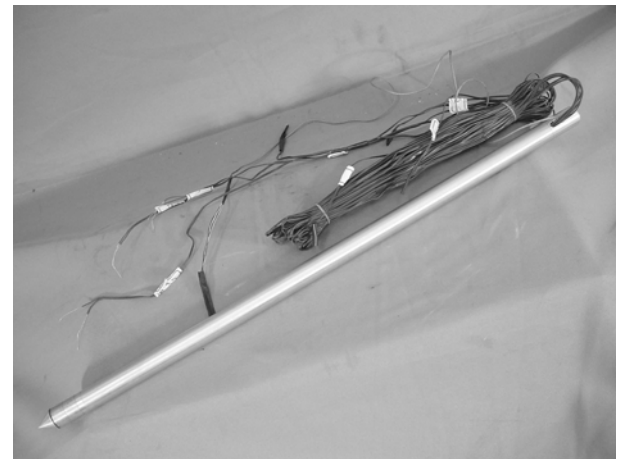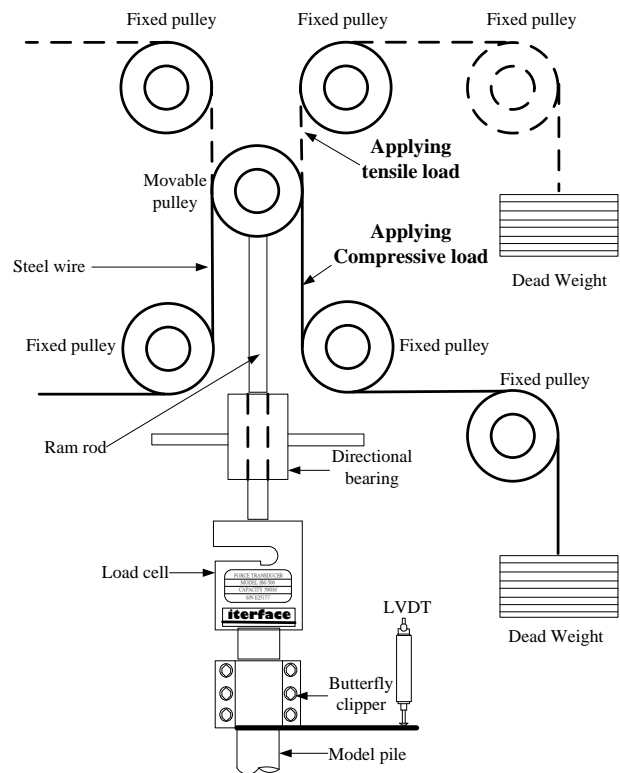

Figure 4 Design of cyclic loading system

2.1.4 Travelling Pluviation Assembly (TPA)

Pluviation is the most common method of preparing sand samples. Its merit is the ability to produce a sample in short time, especially for samples in large calibration chamber and centrifuge. There are two common pluviation methods in the air. One is fixed type pluviation, the other is traveling pluviation. The sand samples produced by fixed type pluviation are often not uniform in relative density and exhibit segregation of different particle sizes. Fretti et al. (1995) reported the sand samples produced by traveling pluviation are more uniform in horizontal and vertical directions as compared to those produced by fixed type pluviation. The lifting height needs to be very small when pluviating one layer, thus the layering effect can be neglected.

To obtain more uniform sand samples, this study used the travelling pluviation assembly designed by Chen (1999). The detailed elements of the assembly are shown in Figure 5, including steel frame, pulley set (providing motion in vertical direction), sand funnel, flexible plastic pipe (pipe diameter=30mm, pipe length=110cm), steel pipes (pipe diameter=10, 12, 14, 16, 18, 21, 25, 30mm, pile length=100mm), and a two- dimensional sliding frame (providing horizontal motions).
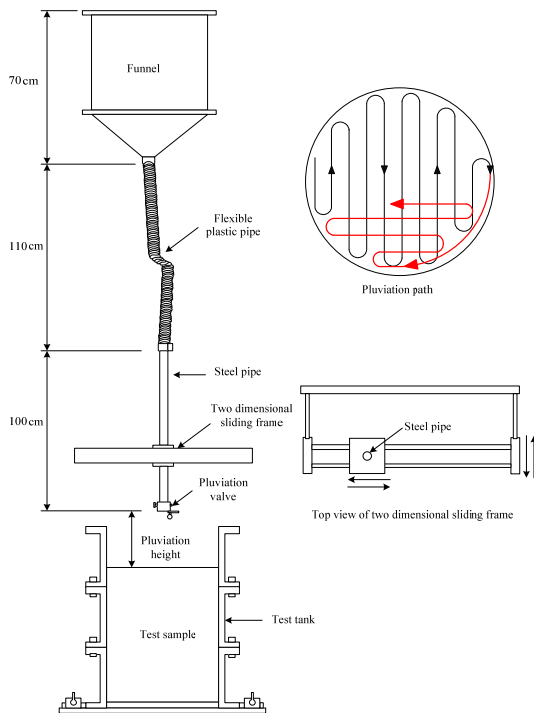

Figure 5 Travelling pluviation assembly (Chen, 1999)

2.2 Sample Preparation and Test Procedure

2.2.1 Sample Preparation

2.2.1.1 Saturated Sand Sample

The saturated sand samples were prepared according to the following procedure:

a. Determine a suitable pipe diameter and pluviation height from the planned relative density (Dr=70% in this study) of sand sample according to the relations of Dr with pipe diameter and pluviation height, as shown in Figure 6. Thus, the steel pipe diameter=12mm and the pluviation height=50cm were selected.

b. Lower the funnel and connect the plastic pipe to the exit of the funnel.

c. Connect steel pipe to the bottom of the plastic pipe and close the bottom valve of the steel pipe preventing sand leakage.

d. Pour test sand into the funnel through the 20# sieve whose function is to retain sand block or impurities, and then lift the

funnel to the suitable height and fix the steel pipe on the two dimensional sliding frame.

e. Put the assembled test tank on the adjustable pulling car. Move the car below the steel pipe and adjust the pluviation height (the distance between the pipe exit to the sample surface) by lifting the car (see Figure 5).

f. Open the valve of the steel pipe to carry out pluviation. The pluviation path is a U-turn type in two directions (see Figure 5). The merit of the U-turn path is to keep the layer surface horizontal and the density uniform so that the pluviation height remains constant.

g. The thickness of each layer is controlled not to exceed the diameter of steel pipe. The pipe exit is closed after finishing one layer pluviation. Adjust the pluviation height to the prescribed height by lowering the car.

h. Repeat step f and g until the sand sample in the test tank reaches the prescribed height.

i. Scrape the extra sands on the tank surface and weigh the sand sample to calculate the dry unit weight and the relative density.

j. Lift the test tank and put it on the platform of the overburden stress loading system, as shown in Figure 7. Then, vacuum air from one hole and pour water slowly from the other hole at the top of test tank to saturate the sample, as shown in Figure 8. A sponge is placed on the top of the sample so that water can slowly seep through the sponge into sand sample to prevent water drops directly on the sand surface causing small caves by impact force of water drop. Carefully control the rate of water drop so that water can seep into the bottom of test tank and force the air in the void of the sand upward until the sample is fully saturated.

k. Start pile penetration after the sand sample is fully saturated for one day.
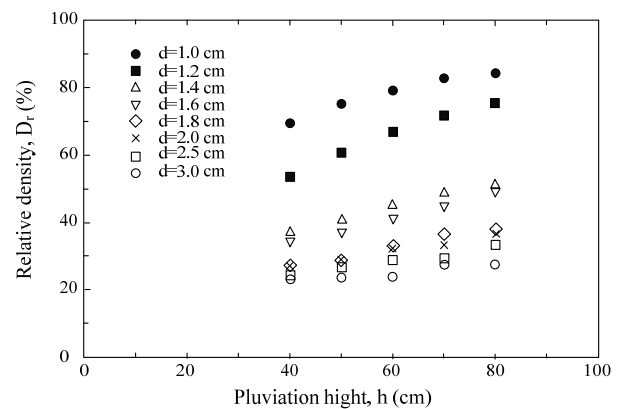
(a) Dr vs. pluviation height
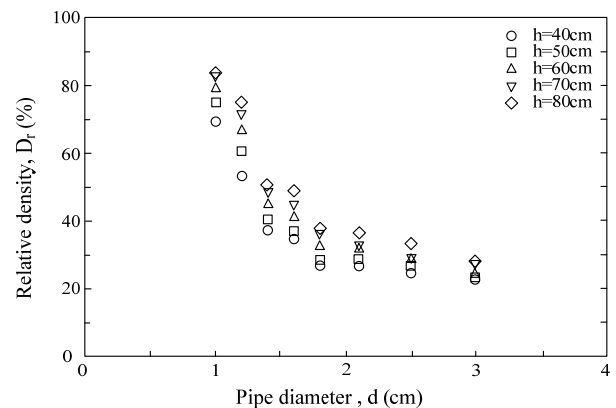
(b) Dr vs. pipe diameter

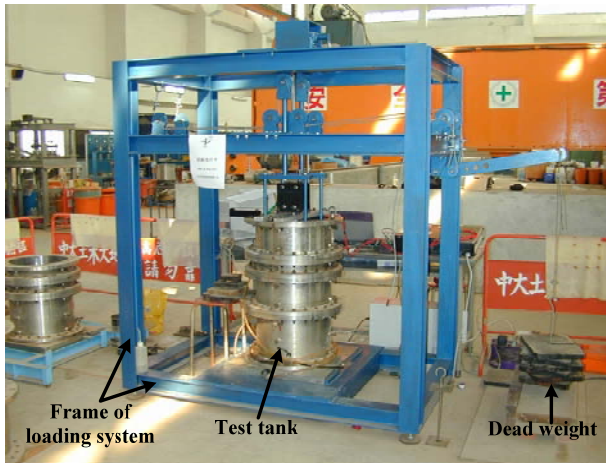Figure 6 Relations of density with pluviation height and pipe diameter in TPA (Chen, 1999)

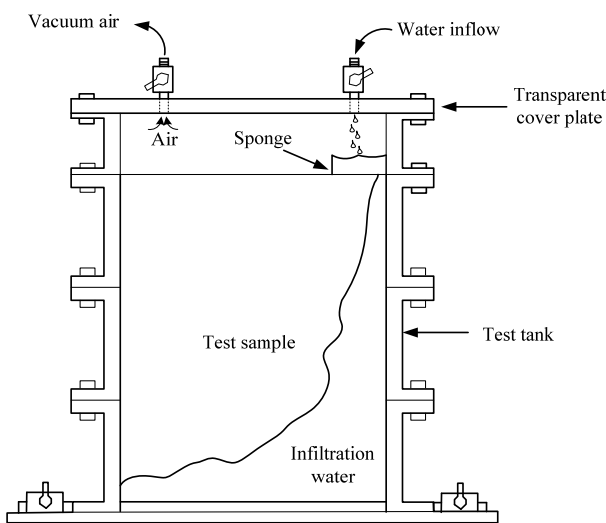Figure 7 The whole model pile test system

Figure 8 Schematic diagram of saturation method

2.2.1.2 Dry Sand Sample

The dry sand samples can be prepared by repeating the above a-i steps, and then, lift the test tank and put it on the platform of the overburden stress loading system to prepare pile penetration.

2.2.2 Calibration Transducers

The transducers used in this model pile load test include the load cells at the top and tip of the model pile, the stain gauges on the pile shaft, the displacement gauge on the pile top. Before test, all the transducers are carefully calibrated to measure their linearity, offset and hysteresis characteristics. Thus, the calibration coefficients of all transducers can be obtained through the calibration work.

2.2.3 Material Properties of Sand and Model Pile

The model pile is made of aluminum alloy 6061-T6 with a density of 26.49 kN/cm^3. A test cylinder of the same material was made in a diameter of 5cm and a height of 6cm. The one dimensional compression test was performed on the test cylinder. Based on the test result, the pile material has a Young's modulus of 60Gpa, a Poisson's ratio of 0.27, and a yielding strength of 275Mpa.

The test sand is a yellow fine sand which was taken from Fulong seashore area in north-eastern corner of Taiwan, thus, commonly called Fulong sand. It is a sub-angular quartz sand with a little feldspar and mica. Table 1 shows its physical properties and particle size characteristics.

2.2.4 Procedure of Pile Load Test

The sand specimens were prepared in a relative density of 70% and with a diameter of 40cm and a height of 60 cm. Two types of cyclic axial load tests were performed for both dry sand and saturated sand.

The first type applies the compressive load incrementally first and then unload incrementally to zero load. After that, apply the uplift load incrementally and then unload incrementally. This finished a compressive-tensile load cycle(C-T type). The same load cycle was then repeated five times.

The second type applies the uplift load incrementally first and then unload incrementally to zero load. After that, apply the compressive load incrementally and then unload incrementally. This finished a tensile-compressive load cycle (T-C type). The same load cycle was then repeated five times also.

Totally, there are four tests in this study, i.e., one C-T and one T-C tests were performed on dry and saturated samples, respectively. Basically, the compressive and the tensile loads are applied and unloaded incrementally as in the traditional static pile load test. The loading procedure refers to ASTM D1143-81 and ASTM D3689-90. Each load cycle is composed of an ultimate compressive pile load test and an ultimate tensile pile load test. The procedures of the compressive and tensile pile load test are described as below:

a. Push the model pile into the prescribed depth in a steady penetration rate and measure the responses of load cell and strain gauges during and after penetration. And then, wait for 24hrs to fully dissipate the excess pore pressure induced by pile penetration. (monitoring the residual load after penetration for dry sand)

b. Install the loading frame, load cell and LVDT on the extended ring of the test tank and then turn on the data logger system.

c. Apply the prescribed load incrementally on the pile top until the settlement of pile top reaches the prescribed settlement, and then unload incrementally to zero loads. The prescribed settlement is selected to be at least greater than 10% of pile diameter, i.e. 1.8 mm of pile. This selection is based on Terzaghi's interpretation criterion which defines the ultimate pile bearing capacity as the pile load corresponding to the settlement of pile top reaching 10% of pile diameter. The load duration of each increment is controlled to approximately 10 minutes and 1.5 minutes for unloading situation by observing whether the settlement is stable or not. If the settlement readings are stable, the next load increment can be applied.

d. Analyze the test records to interpret the cyclic axial bearing behavior of a single pile.

In this study, the measured load-displacement curves of pile head and the transfer curves of the pile shaft were analysed to deduce the characteristics of cyclic axial bearing behaviours, including t-z curves and q-z curves. The focus was put on (1) the difference of the compressive and tensile bearing capacities; (2) the effect of the number of applied load cycles; (3) the development of tip bearing capacity with pile head displacement; (4) the unit friction distribution pattern along pile length.

Table 1 The physical properties of Fulong sand

Soil sample	Fulong sand
Specific gravity	2.65
Effective grain size D_{10} (mm)	0.18
Mean grain size D_{50} (mm)	0.27
Uniformity coefficient $C_u = D_{60}/D_{10}$	1.81
Curvature coefficient $C_c = D_{30}^2/(D_{10} \times D_{60})$	1.07
Maximum dry density (g/cm^3)	1.64
Minimum dry density (g/cm^3)	1.34
Particle shape	subangular
USCS classification	SP

3.   TEST RESULTS AND INTERPRETATION

3.1   Test Results of Dry Sand

3.1.1 C-T Test Results

The real relative density of dry sand is approximately 70% in this test. Figure 9 shows the penetration resistances of pile top and tip with the penetration depth. It can be found the resistances approximately linearly increase with the penetration depth. The maximum resistances occur at the final depth of penetration. The maximum load at the pile top is approximately 725.9 N and the maximum pile tip resistance is approximately 196.2 N (27% of the load at the pile top). The difference of both resistances is approximately 529.7 N which is frictional resistance provided by pile shaft. Figure 10 is the variations of pile axial forces at different positions with depth during penetration. It showed the pile axial forces proportionately decrease from pile top (gauge 1) to pile bottom (gauge 7), and approximately linearly increase with penetration depth. It seems that the pile axial forces are not constantly in linear relation to depth, but have some fluctuations. This is because the pile penetration is operated by manual power with a penetration rate of 0.2 cm/sec so that the penetration rate is not well-controlled. Keep the test system rest for 24 hrs and observe the temperature effect on the transducers. It was found the temperature effect is eliminated by the compensation action of a half bridge connection. After 24hrs waiting, the C-T cyclic load test was performed on the dry sand sample. Figure 11 shows the actual load-displacement curves of pile top during the C-T test. In general, the pile bearing capacity in the first cycle is the greatest, and then decreases with number of loading cycle. The hysteretic loop seems to be stable after the third cycle. The compressive load-displacement curve in the first cycle is a downward concave, which is a typical pattern in a static pile load test. After the first cycle, the compressive load-displacement curve is an upward concave first and becomes a downward concave as displacement becomes large. This is due to the effect of tensile load in the previous cycle. During previous tensile loading, the bottom soil is loosely in contact with the pile tip that will cause large displacement under initial small compressive load in next cycle.
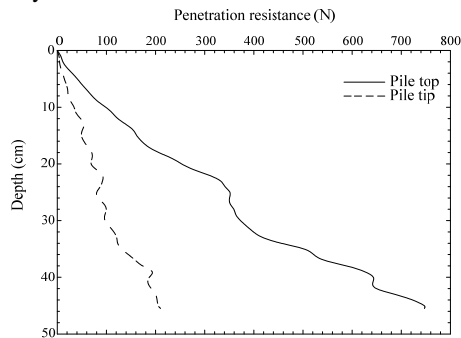

Figure 9 The resistances at the pile top and tip during penetration
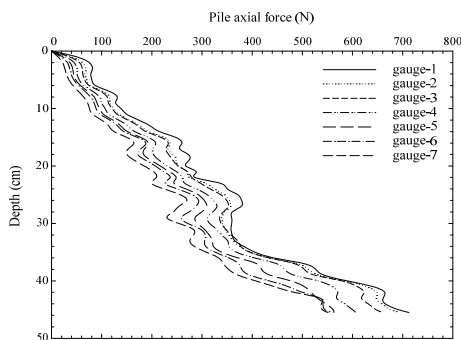

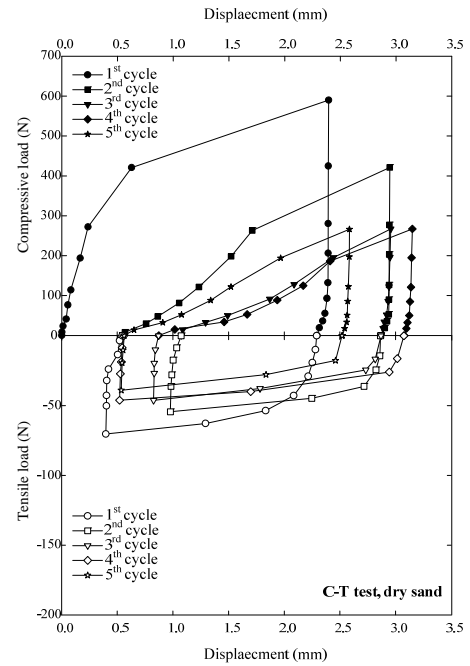Figure 10 The axial forces of pile at different gauges during penetration

Figure 11 The pile top load-displacement curves of cyclic C-T test on dry sand

To more clearly observe the cycle effect, the compressive and tensile load- displacement curves of pile top are displayed in one way direction (no matter the signs of positive or negative), as shown in Figure 12. It shows the compressive resistance is significantly larger than the tensile resistance. If Terzaghi's 0.1D (D=pile diameter) displacement criteria is used to define the ultimate bearing capacity from the load-displacement curve in the first cycle, the ultimate compressive capacity is approximately 519.9 N and the ultimate tensile capacity is approximately 80.4 N, which is only approximately 15% of the compressive capacity.
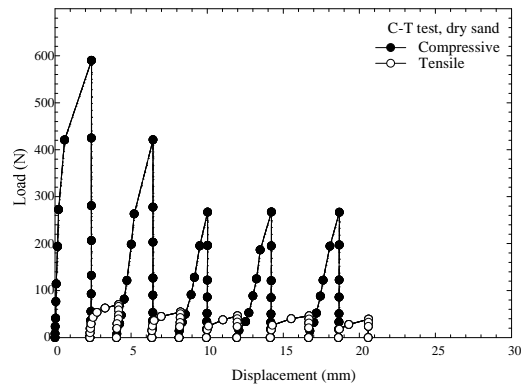

Figure 12 The compressive and tensile load-displacement curves at pile top were compared in the same direction (C-T test, dry sand)

Figure 13 shows the tensile/compressive capacity ratio versus the normalized displacement ratio (pile top displacement/pile diameter) for the five load cycles. It reveals that the tensile/compressive capacity ratio decreases as the displacement ratio increases. For the first cycle, the capacity ratio decreases from 0.25 to 0.13 as the displacement ratio increases from 0.005 to 0.1. The comparison of the compressive load and displacement curves at the pile top and tip for the five cycles are shown in Figure 14. It shows that the resistances at the pile top and tip decrease as the number of load cycle increases, and the resistance of pile tip is approximately 33% of that of pile top in average. Figure 15 shows the relations of the pile tip/top resistance ratio and the normalized displacement ratio (pile head displacement/pile diameter) for the five load cycles. It is

found that the pile tip/top resistance ratio increases as the displacement ratio increases. When the displacement ratio is greater than 0.08, the pile tip/top resistance ratios approach to a converged value of 0.33.
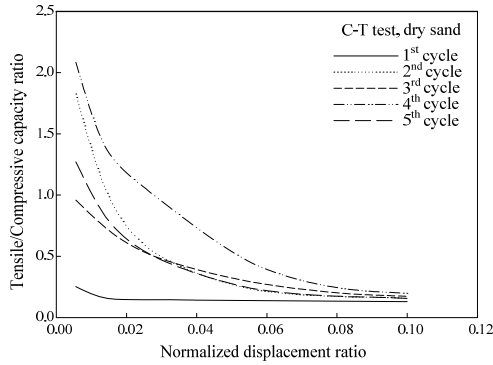

Figure 13 Variation of tensile/compressive capacity ratio with displacement ratio (C-T test, dry sand)
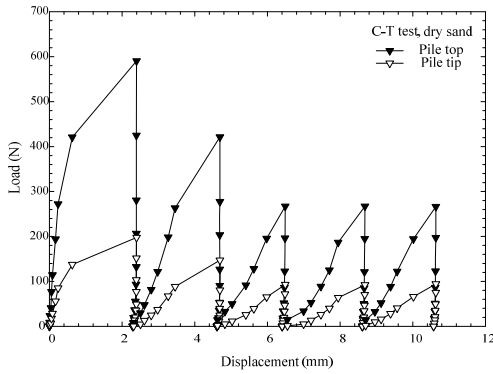

Figure 14 The compressive load-displacement curves at pile top and pile tip (C-T test, dry sand)
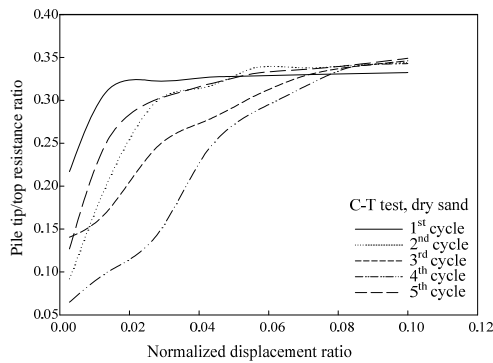

Figure 15 Variation of pile tip/top capacity ratio with displacement ratio (C-T test, dry sand)

Figure 16 shows the distributions of pile axial forces and unit shaft frictions with depth for the compressive load in the first cycle. It is found that axial force distribution is typical and the unit friction in the middle part is larger than those of the upper and lower parts of pile. Figure 17 displayed the distributions of pile axial forces and unit shaft frictions with depth for the tensile load in the first cycle. It is found that axial force at the pile tip is zero and the unit friction increases with depth. The unit friction is the largest around the pile tip. Similar behaviors were also found in the other loading cycles. The average unit friction-relative displacement curves along the interface of soil and pile are commonly called t-z curves. These can be deduced from the distributions of pile axial forces with depth.
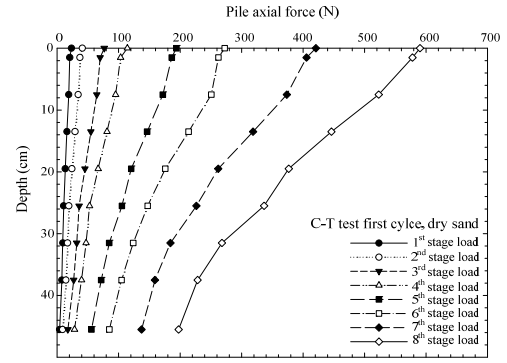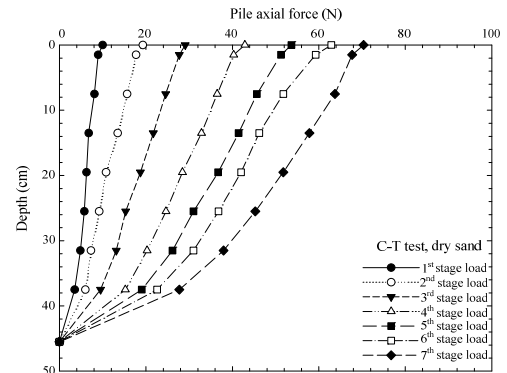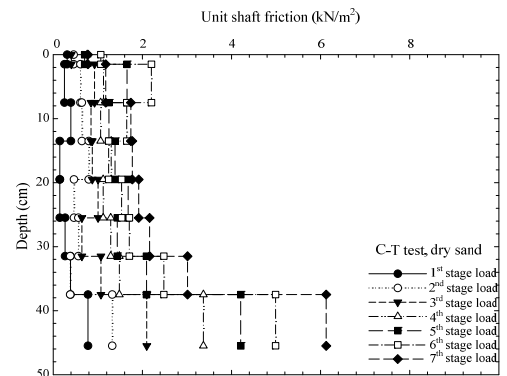

(a)   Pile axial force
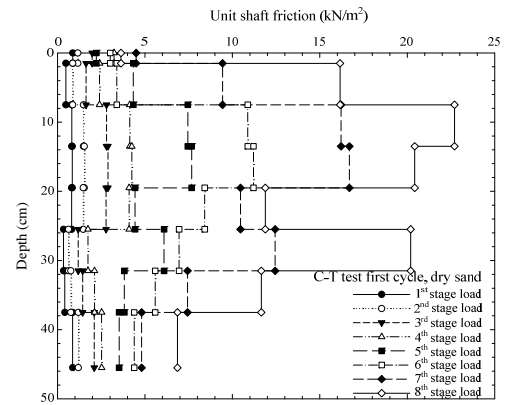
(b)   Unit shaft friction

Figure 16 Variation of pile axial force and unit shaft friction with depth during tensile loading (C-T test, dry sand)


(a)   Pile axial force

(b)   Unit shaft friction

Figure 17 Variation of pile axial force and unit shaft friction with depth during tensile loading (C-T test, dry sand)

Figure 18 shows the t-z curves for compressive and tensile loading for the five cycles. The tensile t-z curves are all concaved down curves. The compressive t-z curve is concaved downward only in the first cycle and they are concaved upward in the second to the fifth cycles. The relation of compressive/ tensile unit friction ratio with the displacement ratio is displayed in Figure 19. It is found that the tensile/compressive unit friction ratio decreases with the increasing displacement ratio. When the displacement ratio reaches 10% of pile diameter, the unit friction ratio converges to a value of 0.25 which is larger than the converged capacity ratio of 0.13. The tensile/compressive unit friction ratio is always larger than the tensile/compressive capacity ratio owing to without considering the contribution of the end bearing part in the compressive loading.
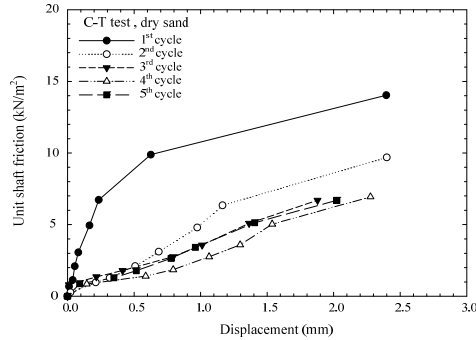
(a)   Compressive t-z curves
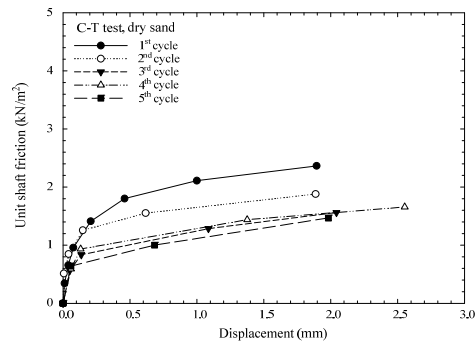
(b)   Tensile t-z curves

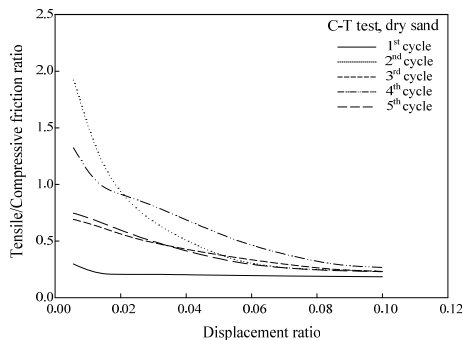Figure 18 The t-z curves of cyclic C-T test on dry sand

Figure 19 Variation of tensile/compressive friction ratio with displacement ratio (C-T test, dry sand)

3.1.2 T-C Test Results

In this test, the relative density of sand sample is also approximately 70%. The pile responses during penetration are similar to the C-T test. Figure 20 shows the actual load-displacement curves of pile top during the T-C test. The tensile bearing capacity in the first cycle is

the greatest, and then decreases with number of loading cycle. However, the compressive load-displacement curves of the five cycles are nearly the same and in a concaved upward shape.
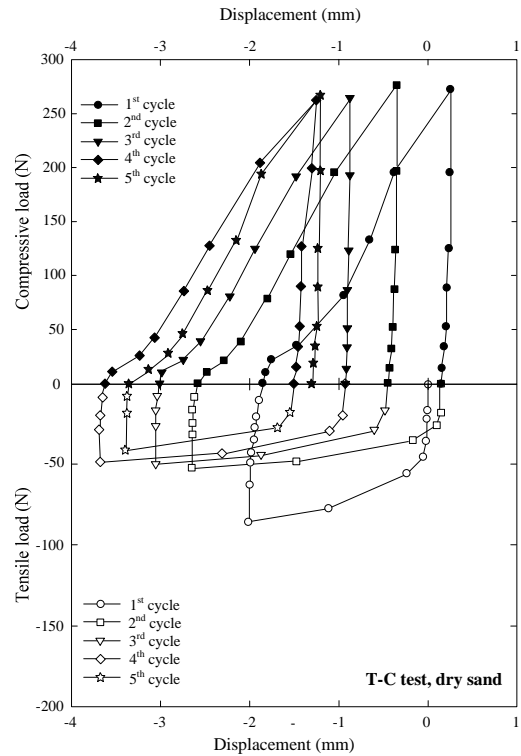

Figure 20 The pile top load-displacement curves of cyclic T-C test on dry sand

The tensile and compressive load-displacement curves of pile top are displayed in one way direction, as shown in Figure 21. It shows the compressive capacity is significantly larger than the tensile capacity. The compressive curves have no cycle effect and the ultimate tensile capacity decreases as the number of loading cycle increases. In the test, the tensile/compressive capacity ratio also decreases as the displacement ratio increases. When the displacement ratio reaches 0.1, the tensile/compressive capacity ratios converge to 0.22 in average. The comparison of the compressive load and displacement curves at the pile top and tip for the five cycles is shown in Figure 22. It shows that the pile tip/top resistance ratio at large displacement is nearly the same. However, it is also found that the pile tip/top resistance ratio increases as the displacement ratio increases. When the displacement ratio is greater than 0.09, the pile tip/top resistance ratios approach to a converged value of 0.27 in average. The distributions of pile axial force and unit friction with depth are similar to those of the previous C-T test.
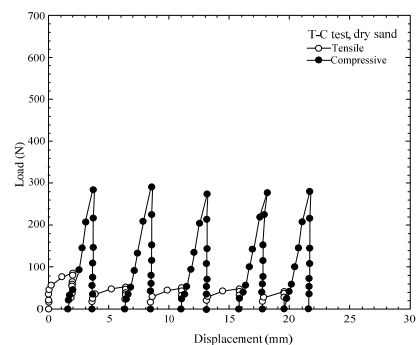

Figure 21 The tensile and compressive load-displacement curves at pile top were compared in the same direction (T-C test, dry sand)

The tensile t-z curves are all concaved downward and the compressive t-z curves are all concaved upward. It is also found that the tensile/compressive unit friction ratio decreases with the increasing displacement ratio. When the displacement ratio reaches 10%, the unit friction ratio converges to a value of 0.4 in average which is larger than the converged capacity ratio of 0.27.
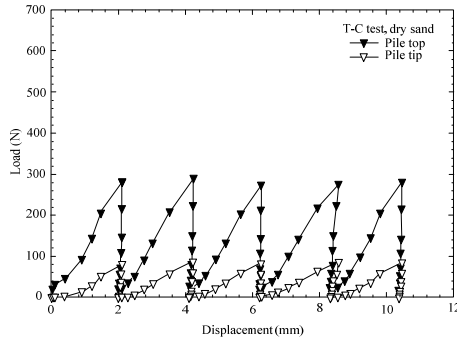

Figure 22 The compressive load-displacement curves at pile top and pile top (T-C test, dry sand)

3.2 Test Results of Saturated Sand

3.2.1 C-T Test Results

In this test, the relative density of the saturated sand sample is approximately 70% and its water content is approximately 30%. The pile responses during penetration are similar to the C-T test in dry sand, except the excess pore pressure over 1 cm height was observed from the standpipe connected to the bottom of the test tank during pile penetration. The excess pore pressure had fully dissipated after 24hrs placement. Figure 23 shows the actual load- displacement curves of pile top during the C-T test. The compressive bearing capacity of the first cycle is the greatest, and then decreases quickly with the number of loading cycle. The same trend is also found for the tensile capacity. The compressive load- displacement curves of the first three cycles are concaved down while they are concaved upward for the last two cycles. The tensile load- displacement curves of five cycles are all concaved downward.
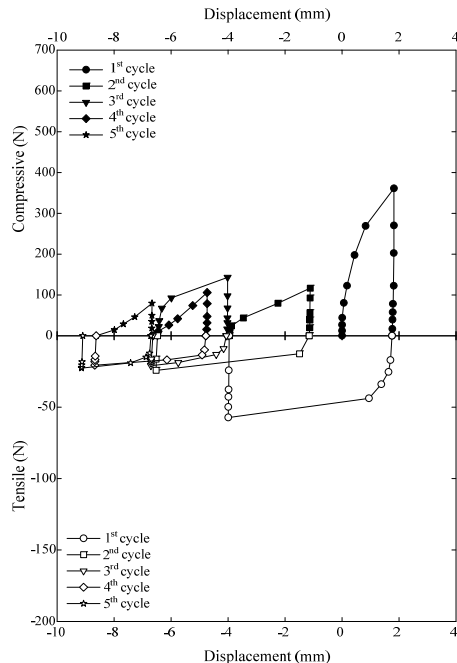

Figure 23 The pile top load-displacement curves of cyclic C-T test on saturated sand

The tensile and compressive load-displacement curves of pile top are displayed in one way direction, as shown in Figure 24. It also shows the compressive capacity is significantly larger than the tensile capacity. Using the Terzaghi's 0.1D criteria, the ultimate compressive and tensile capacities of the first cycle are 343.4 N and 58.9 N respectively which are considerably less than those (519.9 N and 80.4 N of the C-T test of dry sand. In this test, the tensile/compressive capacity ratio also decreases as the displacement ratio increases. When the displacement ratio reaches 0.1, the tensile/compressive capacity ratios converge to 0.23 in average. The comparison of the compressive load and displacement curves at the pile top and tip for the five cycles is shown in Figure 25. It also shows that the pile tip/top resistance ratio increases as the displacement ratio increases. When the displacement ratio is greater than 0.1, the pile tip/top resistance ratios approach a converged value of 0.33 in average. The distributions of pile axial force and unit friction with depth are also similar to the previous C-T test in dry sand. The tensile t-z curves are all concaved downward. The compressive t-z curves of the first three cycles are concaved downward and they are concaved upward for the last two cycles. It is also found that the tensile/compressive unit friction ratio decreases with the increasing displacement ratio. When the displacement ratio reaches 0.1, the unit friction ratios converges to a value of 0.3 in average which is larger than the converged capacity ratio of 0.23.
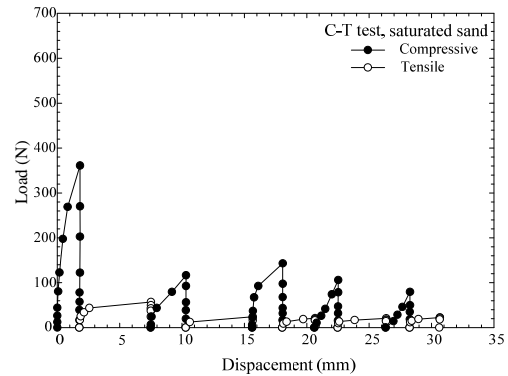

Figure 24 The compressive and tensile load-displacement curves at pile top were compared in the same direction (C-T test, saturated sand)
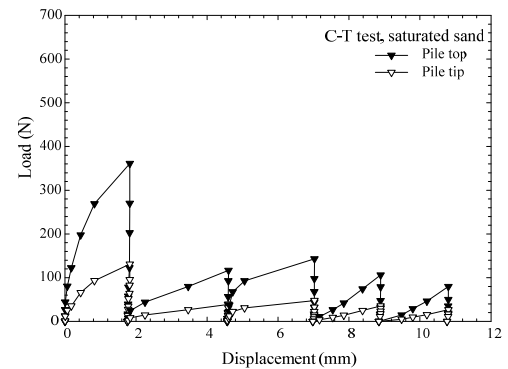
Figure 25 The comparison of compressive load-displacement curves at pile top and pile tip (C-T test, saturated sand)

3.2.2 T-C Test Results

In this test, the relative density of the saturated sand sample is approximately 74% and its water content is approximately 28.5%. The pile responses during penetration are similar to the C-T test in saturated sand. Figure 26 shows the actual load- displacement curves of pile top during the C-T test. The tensile and compressive

bearing capacities of the first cycle are the greatest, and then decrease quickly with the number of loading cycle. The tensile load-displacement curves of five cycles are all concaved downward. The compressive load-displacement curve of the first cycle is concaved down while others are concaved upward for the remaining cycles. The tensile and compressive load-displacement curves of pile top are displayed in one way direction, as shown in Figure 27.

Figure 26 The pile top load-displacement curves of cyclic T-C test on saturated sand

Figure 27 The tensile and compressive load-displacement curves at pile top were compared in the same direction (T-C test, saturated sand)
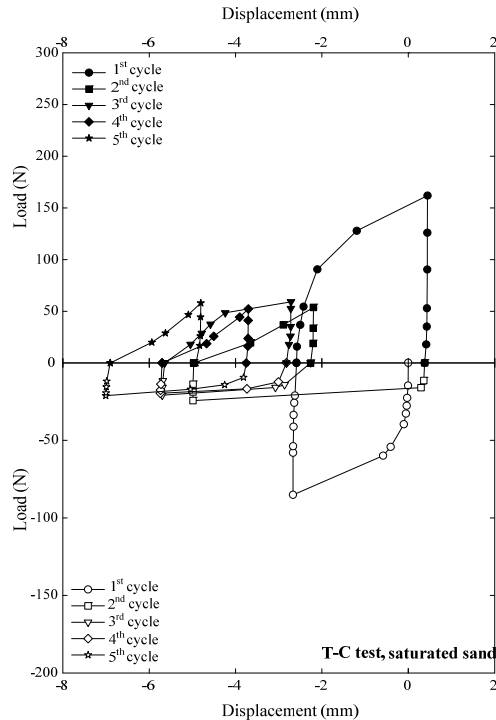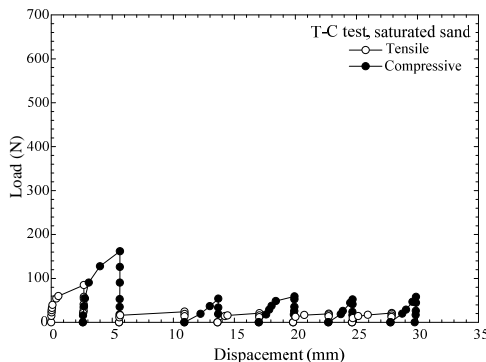
It shows the compressive capacity is significantly larger than the tensile capacity. Using the Terzaghi's 0.1D criteria, the ultimate compressive and tensile capacities of the first cycle are 147.2 N and 73.6 N respectively which are less than those (235.4 N and 83.4 N) of the T-C test of dry sand. In this test, the tensile/compressive capacity ratio also decreases as the displacement ratio increases. When the displacement ratio reaches 0.1, the tensile/compressive capacity ratios converge to 0.5 in average. The comparison of the compressive load and displacement curves at the pile top and tip for the five cycles is shown in Figure 28. It also showed that the pile tip/top resistance ratio increases as the displacement ratio increases. When the displacement ratio is greater than 0.1, the pile tip/top

resistance ratios approach to a converged value of 0.33 in average. The distributions of pile axial force and unit friction with depth are also similar to the previous C-T test in dry sand. The tensile t-z curves are all concaved downward. The compressive t-z curve of the first cycle is concaved down and they are concaved upward for the other cycles. It is also found that the tensile/compressive unit friction ratio decreases with the increasing displacement ratio. When the displacement ratio reaches 0.1, the unit friction ratios converge to an average value of 0.65 which is larger than the converged capacity ratio of 0.5.
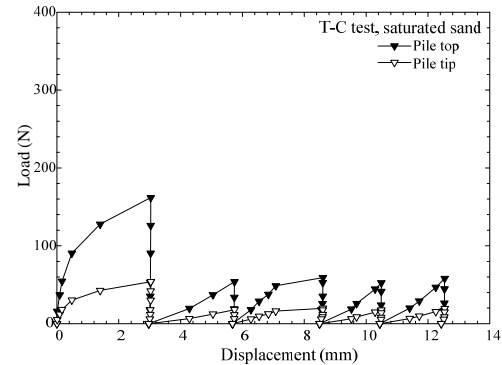

Figure 28 The compressive load-displacement curves at pile top and pile tip (T-C test, saturated sand)

3.3 Analysis

3.3.1 Effect of Sample Saturation

The ultimate compressive and tensile capacities (based on 0.1D criteria) of the first cycle for C-T and T-C load types in both dry and saturated sands are summarized as Table 2 below.

Table 2 The ultimate capacities of the first cycle for C-T and T-C load types

Soil sample	Dry sand		Saturated sand	
Load type (1st cycle)	C-T	T-C	C-T	T-C
Compressive capacity (N)	519.9	235.4	343.4	147.2
Tensile capacity (N)	80.4	83.4	58.9	73.6

In the first cycle, the ultimate compressive capacities of dry sand are significantly higher than those of saturated sand. This results from the initial static water pressure and the excess pore pressure induced by compressive load. The increase of pore pressure decreases the effective stress surrounding the pile, thus causes the reduction of compressive capacity of pile. However, the tensile capacities differ only a little for dry and saturated sands. That is because during the uplift of the pile in saturated sand, there will be a suction pressure occurring in the sand surrounding pile bottom, thus creating the negative excess pore water pressure and increasing the effective stress surrounding the pile. This compensates the effective stress caused by the initial positive static pressure. Therefore, the difference of tensile capacities of dry and saturated sands is very small.

3.3.2 Effect of the Number of Load Cycles

No matter C-T or T-C cyclic load test in dry or saturated sand, the compressive and the tensile capacities generally decrease with the number of load cycle, except in the case of the compressive loading part of the T-C test in dry sand. The pile bearing behavior attains stable conditions mostly after the second cycle for dry and saturated sand. If a capacity softening ratio is defined as the average compressive and tensile bearing capacities in steady cycles divided by those capacities of the first cycle, this ratio represents the

softening effect due to the increasing number of load cycles. Table 3 summarizes the softening ratios in the cyclic pile load tests. It is found that the softening effect is especially significant for saturated sand. In general, the softening ratio can take a value of 0.5-0.6 for dry sand and a value of 0.3-0.5 for saturated sand.

Table 3 The softening ratios deduced from the cyclic axial pile load tests

Soil sample	Dry sand		Saturated sand	
Load type	C-T	T-C	C-T	T-C
Compressive softening ratio	0.50	1.00	0.27	0.40
Tensile softening ratio	0.60	0.60	0.50	0.31

3.3.3 Differences of Tensile and Compressive Capacities

Based on the above test results, the tensile capacity is significantly less than the compressive capacity no matter the test types and soil types. The differences of tensile and compressive capacities can be represented by two ratios, i.e., the tensile/compressive capacity ratio and the tensile/compressive unit friction ratio. The two ratios decrease with the increasing the normalized displacement ratio and converge to constant value when the displacement ratio reaches 0.1. Table 4 displays the tensile/compressive capacity ratio and unit friction ratio at large displacement in the cyclic pile load tests. It is found that the two ratios are very low for dry sand. Only in the T-C test of saturated sand, these two ratios are close to the specified value of design code.

Table 4 The softening ratios deduced from the cyclic axial pile load tests

Soil sample	Dry sand		Saturated sand	
Load type	C-T	T-C	C-T	T-C
Compressive/Tensile capacity ratio	0.13	0.27	0.23	0.50
Compressive/Tensile unit friction ratio	0.23	0.40	0.30	0.65

3.3.4 Development of Tip Bearing Capacity

Based on the above test results, the pile tip/top resistance ratio increases with the increasing normalized displacement ratio during compressive loading. This ratio approaches to a value approximately 0.33 when the displacement of pile top becomes large. The same pile tip/top resistance ratio was also observed during the pile penetration process. During the penetration process, the tip bearing capacity is fully mobilized due to large penetration displacement. Thus, for the model pile with a length ratio approximately 25, the fully mobilized tip bearing capacity is approximately 1/3 of the total ultimate bearing capacity of pile top.

4. CONCLUSIONS AND DISCUSSIONS

This study designed and built a set of model pile load test equipment for static and cyclic loading. The equipment was used to investigate the cyclic axial bearing behavior of a pile in sand. Four cyclic axial pile load tests have been successfully carried out by the equipment. Two tests are for dry sands and the other two are for saturated sands. Based the observation and analysis on the test results, the following preliminary conclusions can be tentatively drawn.

1. The ultimate tensile capacity is significantly less than the ultimate compressive capacity. The tensile/compressive bearing capacity ratio and unit friction ratio significantly vary with the pile head displacement developed. The larger the pile head displacement, the smaller the capacity ratios, and finally approaching to the constant values. Due to the contribution of tip bearing capacity to the compressive capacity, the tensile/compressive unit friction ratio is always larger than the tensile/compressive bearing capacity ratio.

2. The compressive capacity of saturated sand is approximately 2/3 of that of dry sand; however, the tensile capacity of saturated sand is approximately 4/5 of that of dry sand.

3. The load-displacement curves and t-z curves for tensile loads are all concaved down curves. They are mostly concaved down for compressive loads except the T-C case on dry sand. The unit frictions increase significantly from the pile top to the pile bottom for tensile piles, however, the unit frictions at the top and bottom are smaller than those at the middle part for compressive piles.

4. The number of applied cycle considerably reduces the pile ultimate capacity. The smaller the softening ratio, the larger the softening effect. The softening effect of compressive piles is larger than that of tensile piles.

5. For the model pile with a length ratio approximately 25, the fully mobilized tip bearing capacity is approximately 1/3 of the total ultimate compressive bearing capacity of pile.

Since the model pile load tests performed are in one gravity condition, the overburden pressure is too small to simulate the field condition. Thus, the quantitative conclusions in the paper are only for reference. But the qualitative conclusions might reveal some useful knowledge on cyclic axial bearing behavior of pile. It is suggested that the same model pile load tests can be performed in the centrifuge test so that more realistic field stress condition can be attained.

5. REFERENCES

Amira, M., Yokoyama, Y., and Imaizumi, S., "Friction Capacity of Axially Loaded Model Pile in Sand." Soils and Foundations, Vol. 35, No. 1, 1995, pp. 75-82.

Beringen, F. L., Windle, D., and Van Hooydonk, W. R.. "Results of loading tests on driven piles in sand." Recent developments in the design and construction of piles, ICE, London, England, 1979, 213–225.

Chen, H.W.," Centrifuge Modeling Tests on Laterally Loaded Caisson Type Piles in Sandy Slopes," Doctoral Dissertation, National Central University, Jhongli, Taiwan 1999.

Fretti, C. Lo Presti, D.C.E., and Pedroni, S., "A pluvial deposition method to reconstitute specimens well-graded sand," Geotechnical Testing Journal, Vol. 18, No.2, 1995, pp. 292-298.

Fumio, C. T.," Considerations on the mechanism of the tensile bearing capacity of pile in building design," Japanese Geotechnical Society, Foundation Engineering, Vol. 22, No.7, Tokyo, Japan, 1994, pp.26-32.

Japan Road Association, Specifications for Highway Bridges –Part IV: Substructure. Tokyo, Japan ,1996.

Mansure, C. I., and Hunter, A. H. "Pile Test-Arkansas River project." Proceedings, ASCE, Vol. 96, No.SM5, 1970, pp. 1545-1582.

Nicola, A. D., and Randolph, M. F., "Tensile and Compressive Shaft Capacity of Piles in Sand." Journal of Geotechnical Engineering, Vol. 119, No. 12, 1993, pp. 1952-1973.

Tomlinson, M. J., "Pile Design and Construction Practice," Rainbow Bridge Book Co. Ltd., Taipei, 1977.